Enhanced thermoelectric properties in $Bi_2Sr_{2-X}Ba_xCo_2O_y$ ceramics by Ba doping

Berdan ÖZKURT[a,*], M. A. MADRE[b], A. SOTELO[b], M. A. Torres[b]

[a] Department of Natural and Mathematical Sciences, Faculty of Engineering, Tarsus University, 33400 Tarsus, Turkey

[c] Instituto de Ciencia de Materiales de Aragón (CSIC-Universidad de Zaragoza), Mª de Luna 3, 50018 Zaragoza, Spain.

Abstract

$Bi_2Sr_{2-x}Ba_xCo_2O_y$ polycrystalline samples ($0.00 \leq x \leq 0.15$) were prepared through the classical solid-state reaction method. It has been found that Ba-doped $Bi_2Sr_2Co_2O_y$ was obtained as major phase in all samples, based on XRD results. On the other hand, SEM studies have shown the presence of small amounts of secondary phases. The electrical resistivity values of all Ba doped samples decreased when compared to the undoped one, being minimum for the 0.075Ba doped ones. Seebeck coefficient increase with the increasing temperature in all samples, reaching the highest values in the 0.025 Ba doped sample. Finally, power factor has been calculated using the Seebeck coefficient and electrical resistivity values to determine the thermoelectric performances of samples. The maximum PF value of 0.14 mW/K^2 m at 650 ºC was obtained for 0.075Ba doped sample, which is around 25% higher than the undoped sample at the same temperature. All these results clearly show that the thermoelectric properties of the $Bi_2Sr_2Co_2O_y$ system can be improved by Ba doping at optimal values.

Keywords: $Bi_2Sr_2Co_2O_y$; XRD; SEM; Electrical resistivity; Seebeck coefficient; Power factor

* Corresponding author. Tel.: +90 324 600 0033/2611; fax: +90 324 627 4805

E-mail address: berdanozkurt@tarsus.edu.tr

1. Introduction

Thermoelectric (TE) materials are attracting a lot of interest as they ensure the direct energy conversion between heat and electricity [1-2]. Since the use of thermoelectric materials will reduce the problems of climate change caused by the use of excessive fossil fuels on our planet in recent years, studies in this field continue to be very interesting. Especially for energy generation by using waste heat in thermoelectric materials and for the use of these materials in commercial devices, their efficiency should be increased and their high stability should be maintained over a wide temperature range. Among the different TE materials, oxides are characterized by a relatively high conversion efficiency, thermoelectric power factor, and working temperatures. Moreover, they are composed of cheap (when compared to the classical TE materials [3]), environmentally friendly, and abundant elements in the earth crust [4, 5].

In the way to improve the TE oxides performances, it has been shown that the methods used in their preparation are very important for providing high electrical conductivity, without significantly modifying Seebeck coefficient. It is well known that the performance of such materials is characterized by the dimensionless figure of merit (ZT), which is defined as $TS^2/\rho\kappa$ where S is the Seebeck coefficient, ρ the electrical resistivity, κ the thermal conductivity, and T is the absolute temperature [6]. It is obvious from this formula that improving ZT values, increasing the energy transformation efficiency, electrical resistivity and thermal conductivity values should be low, while Seebeck coefficient and working temperatures should be as high as possible. One of the best ways to reduce the electrical resistance, without modifying S, is producing well-oriented grains, which can be easily achieved with texturing techniques such as the laser

floating zone (LFZ) technique [7,8], hot uniaxial pressing [9,10], or spark plasma sintering [11,12]. On the other hand, these characteristics can be also modified by isovalent doping in bulk materials with randomly oriented grains, as shown in previous works [13], without changing the charge carrier concentration. Furthermore, the charge carrier concentration can be also modified by aliovalent doping [14, 15], leading to important improvements of electrical conductivity in these materials.

Other important consideration is related to the crystal structure of the CoO-based TE compounds, which is formed by two alternately stacked layers, a CoO_2 conductive one with CdI_2-type structure, and a block one with rock salt structure. Both layers have the same *a*- and *c*-axis lattice parameters and β angles but different *b*-axis length, causing a misfit along the *b*-direction [16]. It is well known that doping can also modify the lattice parameters of the block layer, directly influencing the Seebeck coefficient values [17].

The aim of this work is studying the modification of thermoelectric performances of $Bi_2Sr_2Co_2O_y$ by isovalent Ba doping at the Sr sites ($Bi_2Sr_{2-X}Ba_xCo_2O_y$ with x=0.00, 0.025, 0.05, 0.075, 0.1, 0.125 and 0.15). The structural and microstructural modifications induced by Ba doping will be evaluated and related to the modifications of the thermoelectric properties.

2. Experimental Procedure

$Bi_2Sr_{2-X}Ba_xCo_2O_y$ (x=0.00, 0.025, 0.05, 0.075, 0.1, 0.125 and 0.15) polycrystalline samples were prepared through the conventional solid state reaction method from Bi_2O_3 (Panreac, 98+%), $SrCO_3$ (Panreac, 98+%), $BaCO_3$ (Panreac, 98+%), and Co_3O_4 (Panreac, 98+%) powders. They were weighed in

the appropriate proportions, mixed using an agate mortar and ball milled at 300 rpm for 30 minutes in water media. After drying the wet powders, they were subjected to a thermal treatment consisting in two different steps: 750 ºC for 12 h and at 800 ºC for 12 h, with an intermediate milling in a ball mill for 2 hours at 300 rpm, in order to produce the total carbonates decomposition before the sintering process. The obtained homogeneous mixture was then pressed into 13 mm diameter pellets under 375 MPa applied pressure, followed by a sintering process at 810 ºC for 24 h, under air, with a final furnace cooling to room temperature, to produce the thermoelectric phase.

X-ray powder diffraction analyses were performed in a Rigaku Ultima IV X-Ray Diffractometer in the range 2θ = 3-60º to determine the phases present in the samples. The surface morphologies were performed on representative samples in a Field Emission Scanning Electron Microscopy (FESEM, Zeiss Merlin). Electrical resistivity and Seebeck coefficient were simultaneously determined by the standart dc four-probe technique in a LSR-3 measurement system (Linseis GmbH), in the steady state mode between 50 and 800 ºC under He atmosphere. Moreover, with the electrical resistivity and Seebeck coefficient data, the power factor has been calculated in order to determine the samples performances.

3. Results and discussion

Fig.1 shows the XRD patterns for all $Bi_2Sr_{2-X}Ba_xCo_2O_y$ samples. The diffraction peaks of all samples fit well with previously reported data for this material [18,19], indicating the presence of Ba doped $Bi_2Sr_2Co_2O_y$ phase as the major one, together with minor peaks (identified with *) associated to $Bi_{0.75}Sr_{0.25}O_y$ secondary phase with ($R\bar{3}mH$') space group [20], and to $Sr_6Co_5O_{14.3}$ (indicated

by ▼) [21]. On the other hand, no Ba based secondary phases have been detected, clearly showing that Ba is entering into the crystal structure of the thermoelectric phase. On the other hand, in spite of the larger diameter of Ba, when compared to Sr, no shift has been detected in the $Bi_2Sr_2Co_2O_y$ peaks, independently of the Ba content.

In Fig. 2, representative SEM micrographs performed on longitudinal surfaces of samples, are presented. As it can be observed in the micrographs, three different contrasts can be identified in the samples (shown by numbers for clarity). EDS analysis of these contrasts have shown that they correspond to different phases, and #1 (grey contrast) is the thermoelectric $Bi_2Sr_{2-X}Ba_xCo_2O_y$ phase appearing as the major one. Moreover, minor secondary phases have been identified as #2, and #3 (white and dark grey contrasts, respectively), corresponding to Bi-Sr-O, and Sr-Co-O compositions, respectively. Consequently, it can be deduced that all Ba is found in the thermoelectric phase, as it has not been detected in any secondary phase. Other interesting features which can be seen in these micrographs is the low amount of porosity in the samples, together with a randomly grain orientation in the bulk materials.

Fig. 3 illustrates electrical resistivity evolution with temperature for all samples. In the graph, it can be observed that electrical resistivity is decreased by Ba doping in the whole measured temperature range. This result is in agreement with previous works, in this kind of compounds, for isovalent substitutions when the substituting cation is larger than the substituted one [13,22]. Furthermore, all samples display metallic-like behavior ($d\rho/dT > 0$) with temperature. On the other hand, electrical resistivity values are decreased with Ba addition up to 0.075, increasing for larger doping. This evolution is due to two competing

effects, the first one is that Ba doping decreases the misfit factor in the crystal structure leading to an enhancement of electrical conductivity [17]; while the second one is associated to the presence of a higher atomic weight cation in the structure, which can act as defects decreasing electrical conductivity by scattering charge carriers. However, He et al. reported that replacing Bi with Ba in $Bi_{2-x}Ba_xSr_2Co_2O_y$ the electrical properties of the system were improved by increasing the Co^{4+}/Co^{3+} ratio [23] and, consequently, the charge carrier concentration. Thus, a similar effect could also contribute in the $Bi_2Sr_{2-x}Ba_xCo_2O_y$ compound if some Bi would be replaced by Ba in the structure. The lowest electrical resistivity value at 650 ºC has been determined in 0.075Ba doped samples (19.5 mΩ cm), which is about 20 % lower than the obtained in undoped ones. As it can be observed in Table 1, these values are around the best reported for textured materials, sintered under oxygen, or by aliovalent substitutions with alkaline metals.

Fig. 4 shows the Seebeck coefficient variation with temperature for all samples. In all samples, the sign of the Seebeck coefficient is positive, indicating a predominant conduction through holes, which means a *p*-type conduction [29,33]. Moreover, all samples display the same behavior and very close values, within the measurement errors, in the whole measured temperature range. The very close S values at nearly room temperature suggest similar concentration of charge carrier concentration for undoped and Ba-doped materials, in agreement with Koshibae's expression [34], and contradicting He et al. work [23]. Furthermore, the values are increased when the temperature rises, which is the typical behavior of metallic or degenerated semiconducting materials when the variation of carrier concentration, effective mass, and Fermi

level, with temperature, is negligible [35]. It is well known that the Seebeck coefficient in inorganic thermoelectric materials can be described as a function of the scattering factor (γ) and carrier concentration (*n*) [36-38], indicating that one of the reasons for the raise of Seebeck coefficient with temperature is due to the increase in the scattering factor [39]. In any case, the highest values at 650 ºC have been measured in 0.025Ba doped samples (170 μV/K), which are slightly higher than those of the other samples. Moreover, when compared to the data shown in Table 1, it is clear that these values are in the order of the best reported ones in this family.

Finally, thermoelectric performances were evaluated through the power factor, PF (= S^2/ρ), which has been calculated using the electrical resistivity and Seebeck coefficient data. Fig. 5 shows the variation of PF with temperature for all samples. As it can be easily observed, all Ba doped samples display higher PF values than the undoped one in the whole measured temperature range. This improvement is due to the lower electrical resistivity of those samples, as the Seebeck coefficient is practically the same for all of them, as previously discussed. Consequently, the highest PF values have been obtained for the 0.075Ba doped samples, which reach their maximum values at 650 ºC (~ 0.14 mW/K^2m), which is about 25% higher than the measured in undoped samples. Moreover, as shown in Table 1, these values are among the best reported for this kind of materials, even if considering textured materials, which usually have larger grain sizes and better grain orientation.

All these results clearly show the possibility to improve thermoelectric properties of $Bi_2Sr_2Co_2O_y$ materials via Ba doping to reach values in the order of the obtained by texturing. This is an important result from the point of view of their

practical applications by avoiding the use of complex, long, and expensive procedures as those associated to the different texturing processes.

4. Conclusions

$Bi_{2-x}Ba_xSr_2Co_2O_y$ samples, with $0.00 \leq x \leq 0.15$, have been successfully prepared through the classical solid state method. XRD analysis has shown that only the thermoelectric phase was present in the samples. However, microstructural studies have detected some minor secondary phases in the samples, together with the typical randomly oriented grains microstructure. Electrical resistivity has been decreased with Ba doping when compared to that measured in the undoped samples. However, due to the associated charge carrier scattering effect, the electrical resistivity decreased for Ba content up to 0.075, increasing for further doping. On the other hand, Seebeck coefficient was not significantly affected by doping. Consequently, the highest power factor values were determined in 0.075Ba doped samples at 650 ºC (~ 0.14 mW/K^2m), which is around 25% higher than that calculated for undoped samples and in the order of the reported for textured materials. These results can help to approach the practical applications of these materials prepared by economical routes and avoiding the long, and expensive processes necessary for texturing them.

Note: The data that support the findings of this study are available from the corresponding author [Berdan Özkurt], upon reasonable request.

Acknowledgements

All samples have been prepared in Department of Materials Science and Metallurgical Engineering in Zaragoza in Spain. XRD analyses have been made

in the Central Research Laboratory (ÇÜMERLAB) in Çukurova University in Adana, as other measurements in this study have been made in Universidad de Zaragoza in Spain.

A. Sotelo, M. A. Madre and M. A. Torres acknowledge the Spanish MINECO-FEDER (MAT2017-82183-C3-1-R) and Gobierno de Aragón-FEDER (Research group T54-20R), for financial support. Authors also acknowledge the use of Servicio General de Apoyo a la Investigación-SAI, Universidad de Zaragoza.

Author Contributions

All authors contributed to the study conception and design. Material preparation, and analysis were performed by [Berdan Özkurt], [Maria Madre], [Andres Sotelo] and [M. A. Torres]. The first draft of the manuscript was written by [Berdan Özkurt] and all authors commented on previous versions of the manuscript. All authors read and approved the final manuscript.

References

[1] Y. Lei, Z. G. Chen, M. S. Dargusch, Z. Jin, High performance thermoelectric materials progress and their applications, Adv. Energy Mater. 8 (2018) 1701797.

[2] D. Champier, Thermoelectric generators: a review of applications, Energy Convers. Manag. 140 (2017) 167-181.

[3] S. LeBlanc, Thermoelectric generators: Linking material properties and systems engineering for waste heat recovery applications, Sust. Mater. Technol. 1-2 (2014) 26-35.

[4] A. A. Yaroshevsky, Abundances of chemical elements in the Earth's crust, Geochem. Int. 44 (2006) 48-55.

[5] J. He, Y. Liu, R. Funahashi, Oxide thermoelectrics: The challenges, progress, and outlook, J. Mater. Res. 26 (2011) 1762-1772.

[6] D. M. Rowe. In: D. M. Rowe, editor. Thermoelectrics handbook: macro to nano. 1st ed. Boca Raton, FL: CRC Press; 2006.

[7] A. Sotelo, S. Rasekh, G. Constantinescu, M. A. Torres, M. A. Madre, J. C. Diez, Improvement of textured $Bi_{1.6}Pb_{0.4}Sr_2Co_{1.8}O_x$ thermoelectric performances by metallic Ag additions, Ceram. Int. 39 (2013) 1597-1602.

[8] G. Constantinescu, S. Rasekh, M. A. Torres, M. A. Madre, J. C. Diez, A. Sotelo, Enhancement of the high-temperature thermoelectric performance of $Bi_2Ba_2Co_2O_x$ ceramics, Scr. Mater. 68 (2013) 75-78.

[9] H. Wang, X. Sun, X. Yan, D. Huo, X. Li, J.-G. Li, X. Ding, Fabrication and thermoelectric properties of highly textured $Ca_9Co_{12}O_{28}$ ceramic, J. Alloy. Compd. 582 (2014) 294-298.

[10] J. C. Diez, S. Rasekh, M. A. Madre, E. Guilmeau, S. Marinel, A. Sotelo, Improved thermoelectric properties of Bi-M-Co-O (M= Sr, Ca) misfit compounds by laser directional solidification, J. Electron. Mater. 39 (2010) 1601-1605.

[11] N. Y. Wu, T. C. Holgate, N. V. Nong, N. Pryds, S. Linderoth, High temperature thermoelectric properties of $Ca_3Co_4O_{9+\delta}$ by auto-combustion synthesis and spark plasma sintering, J. Eur. Ceram. Soc. 34 (2014) 925-931.

[12] J. G. Noudem, D. Kenfaui, D. Chateigner, M. Gomina, Toward the enhancement of thermoelectric properties of lamellar $Ca_3Co_4O_9$ by edge-free spark plasma texturing, Scr. Mater. 66 (2012) 258-260.

[13] F. Delorme, C. Fernandez Martin, P. Marudhachalam, D. Ovono Ovono, G. Guzman, Effect of Ca substitution by Sr on the thermoelectric properties of $Ca_3Co_4O_9$ ceramics, J. Alloy. Compd. 509 (2011) 2311-2315.

[14] W. Gao, G. Wang, X. Li, X. Hu, H. Song, Improved thermoelectric properties of hole-doped $Bi_{2-x}Na_xBa_2Co_2O_y$ ceramics, Int. J. Mod. Phys. B 31 (2017) 1750042.

[15] M. Fan, Y. Zhang, Q. Hu, Y. Zhang, X. J. Li, H. Song, Enhanced thermoelectric properties of $Bi_2Sr_2Co_2O_y$ by alkali metal element doping and SiC dispersion, Ceram. Int. 45 (2019) 17723-17728.

[16] A. Maignan, S. Hebert, M. Hervieu, C. Michel, D. Pelloquin, D. Khomskii, Magnetoresistance and magnetothermopower properties of Bi/Ca/Co/O and Bi(Pb)/Ca/Co/O misfit layer cobaltites, J. Phys.-Condens. Matter 15 (2003) 2711-2723.

[17] Y. Klein, A. Maignan, D. Pelloquin, M. Hervieu, S. Hebert, Thermoelectric power in misfit cobalties ceramics: optimization by chemical substitutions, Bol. Soc. Esp. Ceram. V. 45 (2006) 122-125.

[18] M. Kato, Y. Goto, K. Umehara, K. Hirota, I. Terasaki, Synthesis and physical properties of Bi-Sr-Co-oxides with 2D-triangular Co layers intercalated by iodine, Phys. B 378-380 (2006) 1062-1063.

[19] A. Sotelo, Sh. Rasekh, E. Guilmeau, M. A. Madre, M. A. Torres, S. Marinel, J. C. Diez, Improved thermoelectric properties in directionally grown $Bi_2Sr_2Co_{1.8}O_y$ ceramics by Pb for Bi substitution, Mater. Res. Bull. 46 (2011) 2537-2542.

[20] D. Mercurio, J. C. Champarnaud-Mesjard, B. Frit, P. Conflant, J. C. Boivin, T. Vogt, Thermal evolution of the crystal structure of the rhombohedral $Bi_{0.75}Sr_{0.25}O_{1.375}$ phase: a single crystal neutron diffraction study, J. Solid State Chem. 112 (1994) 1-8.

[21] K. Iwasaki, H. Yamane, T. Murase, M. Yoshino, T. Ito, T. Nagasaki, Y. Arita, T. Matsui, Crystal structure of an oxygen deficient strontium cobaltate, $Sr_6Co_5O_{14.3}$, J. Ceram. Soc. Jpn. 117 (2009) 89-93.

[22] M. A. Torres, F. M. Costa, D. Flahaut, K. Touati, Sh. Rasekh, N. M. Ferreira, J. Allouche, M. Depriester, M. A. Madre, A. V. Kovalevsky, J. C. Diez, A. Sotelo, Significant enhancement of the thermoelectric performance in

$Ca_3Co_4O_9$ thermoelectric materials through combined strontium substitution and hot-pressing process, J. Eur. Ceram. Soc. 39 (2019) 1186-1192.

[23] Q. L. He, Z. Qin, J. Zhang, F. Gao, X. Hu, H. Z. Song, Enhanced Thermoelectric Properties of Hole-Doped $Bi_{2-x}Ba_xSr_2Co_2O_y$ Ceramics, J. Electron. Mater. 43 (2014) 1432-1435.

[24] Sh. Rasekh, F. M. Costa, N. M. Ferreira, M. A. Torres, M. A. Madre, J. C. Diez, A. Sotelo, Use of laser technology to produce high thermoelectric performances in $Bi_2Sr_2Co_{1.8}O_x$, Mater. Design 75 (2015) 143-148.

[25] W. Shin, N. Murayama, Thermoelectric properties of (Bi,Pb)-Sr-Co-O oxide, J. Mater. Res. 15 (2000) 382-386.

[26] H. Itahara, C. Xia, J. Sugiyama, T. Tani, Fabrication of textured thermoelectric layered cobaltites with various rock salt-type layers by using β-$Co(OH)_2$ platelets as reactive templates, J. Mater. Chem. 14 (2004) 61-66.

[27] T. Itoh, I. Terasaki, Thermoelectric properties of $Bi_{2.3-x}Pb_xSr_{2.6}Co_2O_y$ single crystals, Jpn. J. Appl. Phys. 39 (2000) 6658-6660.

[28] M. A. Madre M. A. Torres, Sh. Rasekh, J. C. Diez, A. Sotelo, Improvement of thermoelectric performances of $Bi_2Sr_2Co_{1.8}O_x$ textured materials by Pb addition using a polymer solution method, Mater. Lett. 76 (2012) 5-7.

[29] J. J. Shen, X. X. Liu, T. J. Zhu, X. B. Zhao, Improved thermoelectric properties of La-doped $Bi_2Sr_2Co_2O_9$-layered misfit oxides, J. Mater. Sci. 44 (2009) 1889-1893.

[30] G. C. Karakaya, B. Ozcelik, M. A. Torres, M. A. Madre, A. Sotelo, Effects of K substitution on thermoelectric and magnetic properties of $Bi_2Sr_2Co_2O_y$ ceramic, J. Mater. Sci. Mater Electron 28 (2017) 12652-12659.

[31] G. C. Karakaya, B. Ozcelik, M. A. Torres, M. A. Madre, A. Sotelo, Effect of Na-doping on thermoelectric and magnetic performances of textured $Bi_2Sr_2Co_2O_y$ ceramics, J. Eur. Ceram. Soc. 38 (2018) 515-520.

[32] U. Hira, N. Pryds, F. Sher, Thermoelectric Properties of Dual Doped $Bi_2Sr_2Co_2O_y$-Based Ceramics, J. Electron. Mater. 48 (2019) 4618-4626.

[33] R. Funahashi, M. Shikano, $Bi_2Sr_2Co_2O_y$ whiskers with high thermoelectric figure of merit, Appl. Phys. Lett. 81 (2002) 1459-1461.

[34] W. Koshibae, K. Tsuitsui, S. Maekawa, Thermopower in cobalt oxides, Phys. Rev. B 62 (2000) 6869-6872.

[35] D. Flahaut, J. Allouche, A. Sotelo, Sh. Rasekh, M. A. Torres, M. A. Madre, J. C. Diez, Role of Ag in textured-annealed $Bi_2Ca_2Co_{1.7}O_x$ thermoelectric ceramic, Acta Mater. 102 (2016) 273-283.

[36] H. Q. Liu, X. B. Zhao, T. J. Zhu, Y. J. Gu, Thermoelectric properties of $Yb_xCo_4Sb_{12}$ system, J. Rare Earths 30 (2012) 456-459.

[37] H. Q. Liu, H. L. Gao, Y. J. Gu, X. B. Zhao, Effect of Y-filling on thermoelectric properties of $CoSb_3$, J. Rare Earths 29 (2011) 596-598.

[38] F. Zhang, Q. Lu, T. Li, X. Zhang, J. Zhang, X. Song, Preparation and thermoelectric transport properties of Ba-, La- and Ag doped $Ca_3Co_4O_9$ oxide materials, J. Rare Earths 31 (2013) 778-783.

[39] K. Hasezaki, T. Hamachiyo, M. Ashida, T. Ueda, Y. Noda, Thermoelectric properties and scattering factors of finely grained Bi_2Te_3-related materials prepared by mechanical alloying, Mater. Trans. 51 (2010) 863-867.

Figure captions

Fig. 1 Powder XRD patterns for all samples.

Fig. 2. Representative SEM micrographs obtained on surfaces of $Bi_2Sr_{2-x}Ba_xCo_2O_y$ samples for x = a) 0; b) 0.025; c) 0.075; and d) 0.125. The numbers indicate the different phases: #1 thermoelectric; #2 Bi-Sr-O; and #3 Co-Sr-O.

Fig. 3. Resistivity evolution with temperature as a function of Ba content in $Bi_2Sr_{2-x}Ba_xCo_2O_y$ samples.

Fig. 4. Temperature dependence of Seebeck coefficient as a function of Ba content in $Bi_2Sr_{2-x}Ba_xCo_2O_y$ samples.

Fig. 5. Temperature dependence of the power factor as a function of Ba content in $Bi_2Sr_{2-x}Ba_xCo_2O_y$ samples.

Figure 1

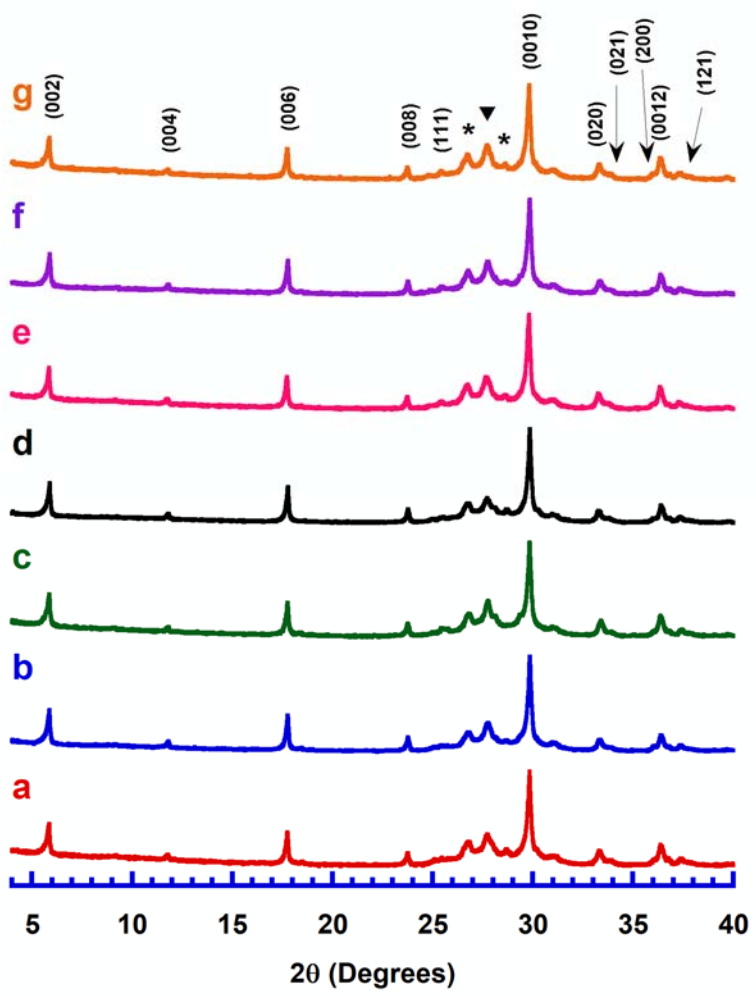
g
(002)
(004)
(006)
(008)
(111)
*
▼
*
(0010)
(020)
(021)
(200)
(0012)
(121)
f
e
d
c
b
a
5
10
15
20
25
30
35
40
2θ (Degrees)

Figure 2

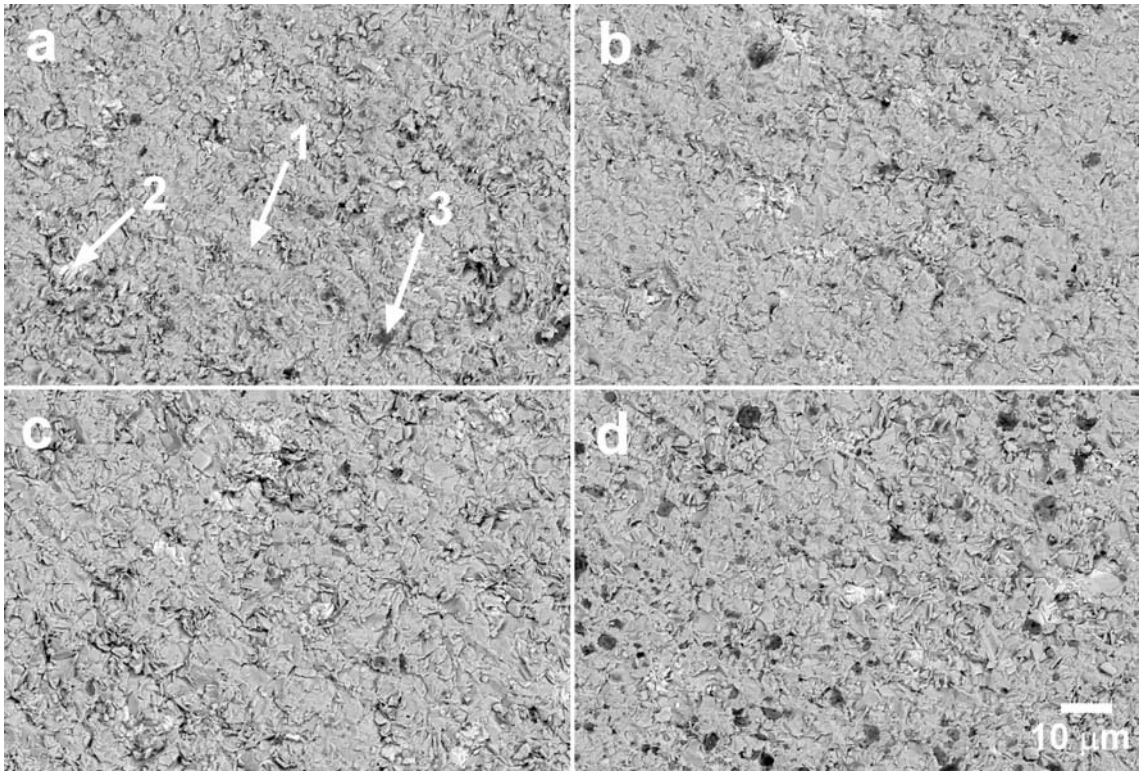

Figure 3

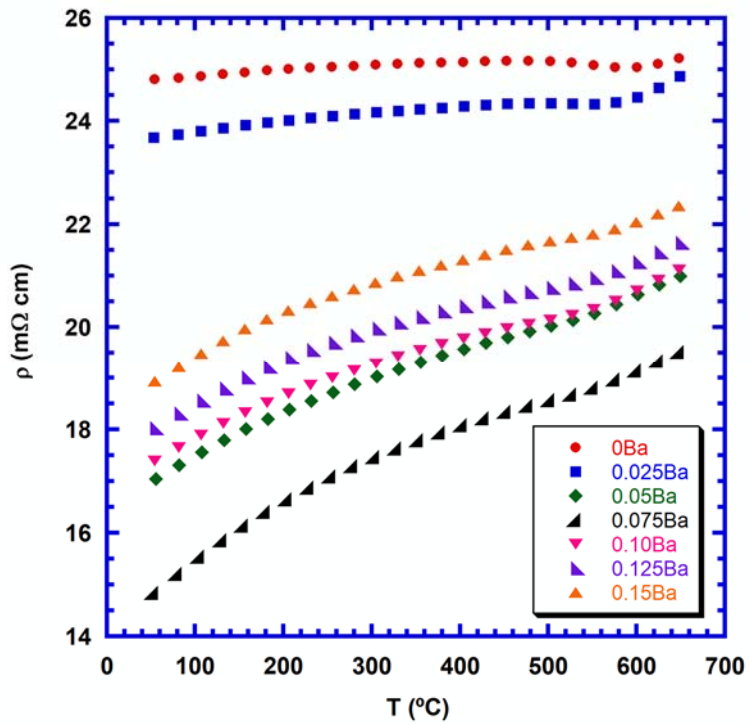
26
24
22
20
18
16
14
ρ (mΩ cm)
0
100
200
300
400
500
600
700
T (°C)
0Ba
0.025Ba
0.05Ba
0.075Ba
0.10Ba
0.125Ba
0.15Ba

Figure 4

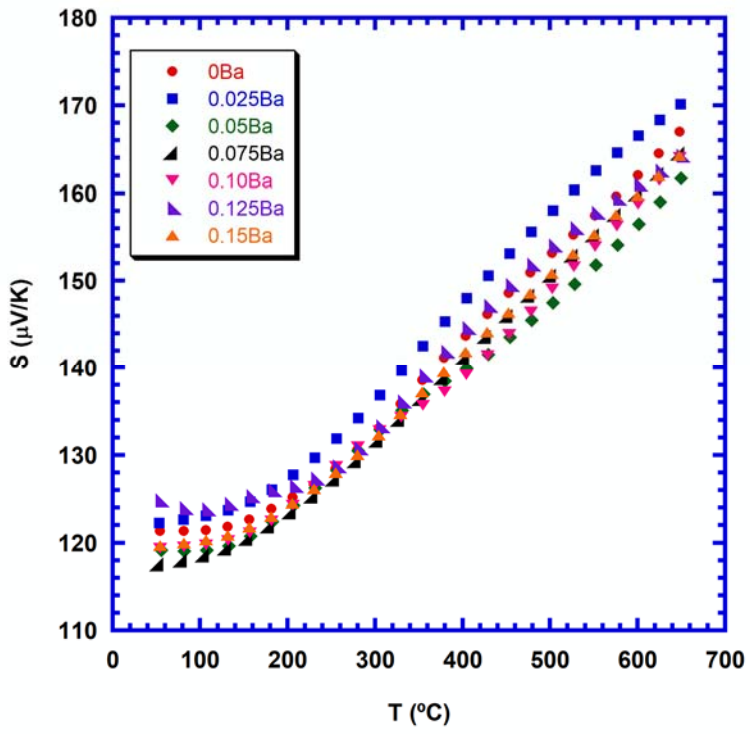
0Ba
0.025Ba
0.05Ba
0.075Ba
0.10Ba
0.125Ba
0.15Ba
S (μV/K)
T (°C)
180
170
160
150
140
130
120
110
0
100
200
300
400
500
600
700

Figure 5

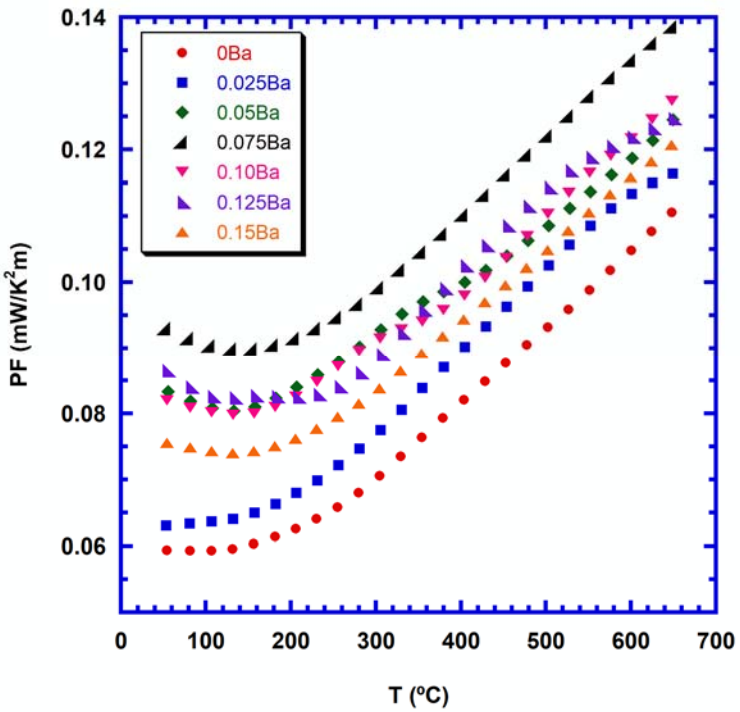
0Ba
0.025Ba
0.05Ba
0.075Ba
0.10Ba
0.125Ba
0.15Ba
PF (mW/K²m)
T (ºC)
0.14
0.12
0.10
0.08
0.06
0
100
200
300
400
500
600
700